Semiconductor Optoelectronics
ISSN: 1001-5868

ACTIVE AND REACTIVE POWER CONTROL IN TRANSMISSION LINE WITH GWO OPTIMIZED PI CONTROLLED FIVE LEVEL UPFC

R. Jayachandra[1] & Dr. G. Tulasi Ram Das[2]
[1] Research Scholar, 2 Professor
[1,2] Department of Electrical and Electronics Engineering [1,2] Jawaharlal Nehru Technological University Hyderabad.

Abstract—In this paper, Grey Wolf Optimization (GWO)optimized PI controlled five level UPFC is proposed for a double circuit transmission line. The most versatile of the FACTS devices, is the Unified Power Flow Controller (UPFC). With a UPFC it is possible to control the balance of the transmitted power between transmission lines, thereby optimizing the use of a transmission grid. This paper introduces decoupled linear UPFC power controllers to obtain the reference ac voltages and currents for the two back-to-back-connected three-phase five-level NPC converters that enforce active and reactive power control in the transmission line. This paper proposes three main contributions to increase the dc-link voltage steadiness of multilevel UPFCs under line faults: 1) decoupled active and reactive linear power controllers; 2) real-time PWM generation; and 3) balancing of dc capacitor voltages. The MATLAB/SIMULINK model for the proposed circuit with GWO-optimized PI controlled five level UPFC is shown here with the results.

Keywords —unified power-flow controller (UPFC), Grey Wolf Optimization, power flow, power flow controller, and FACTS

I.INTRODUCTION

In recent years, environmental, right-of-way, and cost concerns have delayed the construction of both power stations and new transmission lines, while the demand for electronic energy has continued to grow in many countries. This situation has spurred interest in providing already-existing power systems with greater operating flexibility and better utilization. The flexible ac transmission systems (FACTS) concept [1], based on applying leading-edge power electronics technology to existing ac transmission systems, improves stability to increase usable power transmission capacity to its thermal limit. A unified power flow controller (UPFC) [2]–[3], which is one of the most promising devices in the FACTS concept, has the potential of power flow control and/or voltage stability in power transmission systems. Flexible AC transmission system is an evolving technology-based solution to help electric utilities fully utilize their transmission assets. Its first concept was introduced by N.G Hingorani, in 1988[4]. Since then different kinds of FACTS devices have been proposed. Among them, the UPFC is the most versatile and effective device which was introduced in 1991[5].

The UPFC consist of voltage source converters, one connected in series and other in shunt and both are connected back to back through a D.C capacitor [6]. In order to investigate the impact

of UPFC on power systems effectively, it is essential to formulate their correct and appropriate model. In the area of power flow analysis models of the UPFC have been published[7] which treat the UPFC either as one series voltage source and one shunt current source model or both the series and the shunt are represented by voltage sources. in [8] presented a decoupled model which is simple to implement but it presents some restrictions. In [9] the UPFC is represented by two voltage sources called the voltage source model (VSM) discusses the distinguishing features of the voltage source model at length.[10] introduced another model called the power injection models (PIM). Taking these two models as the base models, few other models [11] have been developed with slight modifications in order to circumvent the limitations of the base models.

In [12] two machine model systems with SSSC have been taken into consideration and simulated using MATLAB/SIMULINK. In order to optimize the parameters of voltage and active, reactive power flow in the line, PI control technique using SSSC model has been introduced. A comparison of these parameters between compensated and uncompensated line have been carried out and the results indicate that the distortion is at satisfactory level. In[13] UPFC performance and control methods were proposed for regulating the flow of power. In order to improve the flow of power over a transmission line in a typical IEEE-14 bus test system, this study demonstrates real power flow regulation across a transmission line using UPFC and the result was positive.

The effectiveness of UPFC is examined in [14] for regulating flow of power over a transmission line. In order to improve real and reactive power flow control over a transmission line, UPFC is used and simulated in this research and the results obtained are effective and encouraged. In [15] this essay discuss about User-Defined Modeling (UDM) based framework for UPFC model. Additionally, under the assumption of a two-machine system, the characteristics of steady-state and dynamic responses are compared and studied. The feasibility and effectiveness of the suggested UPFC in terms of the independent management of power flow and improvement of transient stability are supported by numerical results from numerous simulations and the results are encouraged and effective.

The most versatile of the FACTS devices, is the Unified Power Flow Controller (UPFC). With a UPFC it is possible to control the balance of the transmitted power between transmission lines, thereby optimizing the use of a transmission grid. A UPFC does this by injecting a controlled series voltage on a transmission line. In (1), active and reactive power P, Q transported by an ideal purely inductive transmission line are given, in the function of sending and receiving end voltages u_s1, u_s2, line impedance X, and phase angle ρ. This is a commonly used model for overhead transmission lines of short length, whose impedance is mainly inductive [16], [17]. As a UPFC can control the sending end voltage u_s1, phase angle ρ, and line impedance X, it can adequately control active and reactive power flow on a transmission line.

$$P = \frac{u_{s1}u_{s2}\sin\rho}{X}, Q = \frac{u_{s1}^2 - u_{s1}u_{s2}\cos\rho}{X} \quad (1)$$

To enhance UPFC performance, a different approach is considered here. It uses simplified power system models to derive the decoupled power controllers, but detailed modeling of the UPFC power converters improves their ride-through capability. This paper introduces decoupled linear UPFC power controllers to obtain the reference ac voltages and currents for the two back-to-back-connected three-phase five-level NPC converters that enforce active and reactive power in the transmission line. The NPC converters share common dc-link capacitor C(Fig. 1) and rely on real-time PWM generators to enforce the shunt converter ac input currents and series converter line-to-neutral voltages. The dc-link voltage is regulated by the shunt converter, while shunt and series converters balance the dc voltages of the dc-link capacitors. Real-time PWM generation and the double balance of the four dc capacitor dc voltages have been shown to enhance the voltage ride-through capability. Simulation results are presented to show the active and reactive power control.

To optimize the gains of the PI controller used in the control system, GWO optimization is adopted. Grey Wolf Optimization (GWO), first introduced by Kennedy and Eberhart, is one of the modern heuristic algorithms. It was developed through the simulation of a simplified social system and has been found to be robust in solving continuous nonlinear optimization problems [18]. The GWO technique can generate a high-quality solution within a shorter calculation time and stable convergence characteristics than other stochastic methods..The effectiveness of the proposed methods is compared to controllers without real-time PWM generation and decoupled active and reactive power control.

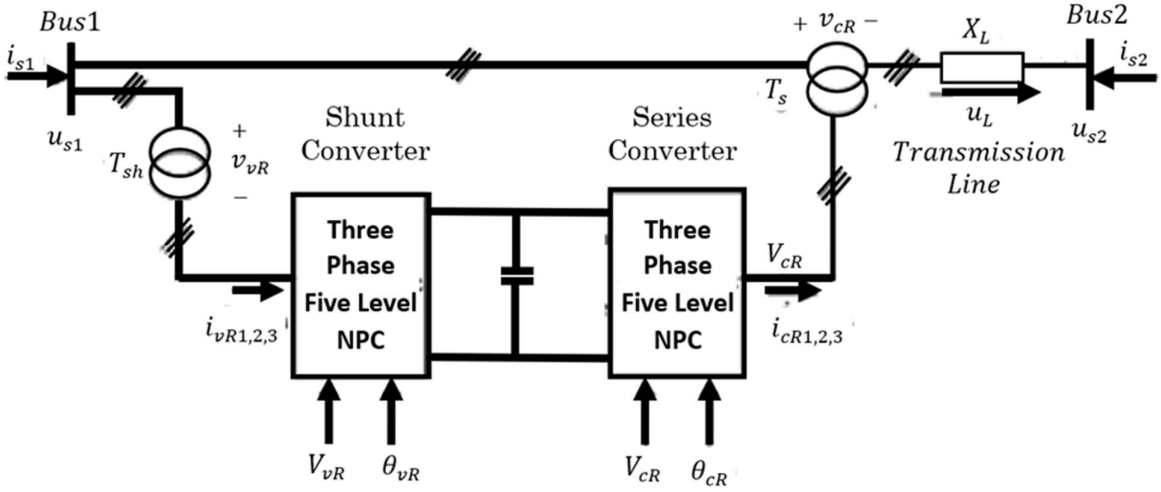

Fig.1. Typical Diagram Configuration of the UPFC

II.UPFC DECOUPLED POWER CONTROL

Fig. 1 shows the typical diagram configuration of the UPFC two high-power back-to-back NPC multilevel voltage-source inverters connected through a smoothing capacitor bank dc-link voltage. Oscillation damping control uses UPFC nonlinear control schemes. Unified power flow controller is a generalized synchronous voltage source, represented at the fundamental frequency by voltage phasor u with controllable magnitude u ($0 \leq u \leq u\_max$) and angle α ($0 \leq \alpha \leq 2\pi$), in series with the transmission line. The UPFC consists of two voltage-sourced inverters. These back-to-back inverters are operated from a common DC link provided by a DC storage capacitor. This arrangement functions as an ideal ac-to-ac power inverter in which

the real power can freely flow in either direction between the ac terminals of the two inverters, and each inverter can independently generate (or absorb) reactive power at its own ac output terminal. The series inverter provides the main function of the UPFC by injecting a voltagewith controllable magnitude u and phase angle α in series with the line via an insertion transformer. This injected voltage acts essentially as a synchronous ac voltage source. The transmission line current flows through this voltage source resulting in reactive and active power exchange between it and ac system. The inverter generates the reactive power exchanged at the ac terminal internally. The active power exchanged at the ac terminal is converted into dc power, which appears at theDC link as a positive or negative real power demand.

The basic function of shunt inverter is to supply or absorb the real power demanded by series inverter at the common DC link to support the real power exchange resulting from series voltage injection. This DC link demand of series inverter is converted back to ac by shunt inverter and coupled to the transmission line bus via a shunt-connected transformer. In addition to this the shunt inverter can also generate or absorb controllable reactive power, if it is desired and thereby provides independent shunt reactive compensation for the line. The three main control parameters of UPFC are magnitude (u), angle (α) and shunt reactive current control of real and reactive power can be achieved by injecting series voltage with appropriate magnitude and angle. This injected voltage is transformed into dq reference frame, which is split into u_d and u_q . These coordinates can be used to control the power flow. The controllers for UPFC shunt and series branch VSIs are described below.

Active and reactive PF can be controlled by injecting a Voltage with variable magnitude and phase angle through a step-up series coupling transformer Ts (Fig. 1), using the series converter line-to-neutral voltages, so that ,where is the series transformer voltage ratio. The shunt converter provides the UPFC-needed active power and usually controls the shunt reactive power. In steady state, the active power exchanged between the UPFC and the power system is close to zero, meaning constant dc-link voltage. The multilevel shunt converter input currents are controlled in the reference frame, so that the component keeps the dc voltage constant, while the component regulates the shunt reactive power. To obtain the UPFC decoupled active and reactive power controllers and assuming a balanced three-phase system, a simplified per-phase model of the transmission system as in Fig. 2 is considered, where line transversal and generator impedances were neglected when compared to the longitudinal impedance variations during line interruptions. Also, assuming controllers enforce fast dynamics, dc-link voltage disturbances can be neglected, together with power semiconductor switching dynamics. Therefore, the UPFC can be ideally represented as a controlled series voltage source and a controlled shunt current source. Using this equivalent circuit, the approximate dynamics of the three-phase currents in the transmission line are

$$\frac{di_k}{dt} = \frac{u_{k1} - R_{ik} + v_{cR} - u_{k2}}{L} \text{ for k} = 1, 2, 3 \tag{2}$$

Using Park transformation, the dynamics in the space are

$$L\frac{d}{dt}\begin{bmatrix} i_d \\ i_q \end{bmatrix} = \begin{bmatrix} -R & \omega L \\ -\omega L & -R \end{bmatrix}\begin{bmatrix} i_d \\ i_q \end{bmatrix} + \begin{bmatrix} u_{Ld} \\ u_{Lq} \end{bmatrix} \tag{3}$$

$$u_{Ld} = u_{1d} + u_{cRd} + u_{2d} \tag{4}$$

$$u_{Lq} = u_{1q} + u_{cRq} + u_{2q} \tag{5}$$

Voltages v_{cRd}andv_{cRq} were obtained by applying Park's transformation to the step-up converted voltages $v_{\mathrm{cR}\alpha} = \mathrm{N_c V_{cR}}\propto$ and $v_{\mathrm{cR}\beta} = \mathrm{N_c V_{cR}}\beta$.

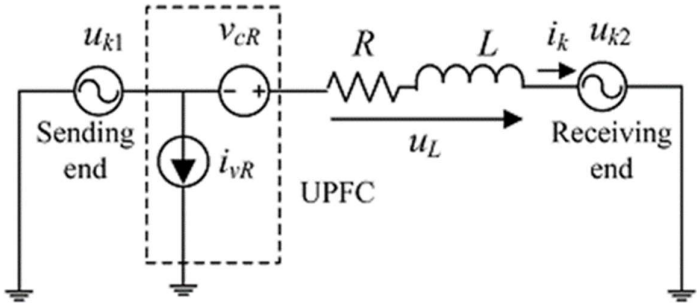

Fig.2. Equivalent circuit of a transmission system with UPFC

The Unified Power Flow Controller (UPFC) was devised for the real-time control and dynamic compensation of ac transmission systems, providing multi-functional flexibility required to solve many of the problems facing the power delivery industry.

From the conceptual viewpoint, the UPFC is a generalized synchronous voltage source (SVS), represented at the fundamental (power system) frequency by voltage phasor u_pq with controllable magnitude u_pq(0 ≤u_pq ≤ u_pqmax) and angle ρ(0≤ρ≤2π), in series with the transmission line, as illustrated for an elementary two-machine system (or for two independent systems with a transmission link intertie) in Figure 2. In this arrangement the SVS generally exchanges both reactive and real power with the transmission system. Since, by definition, an SVS can generate only the reactive power exchanged, the real power must be supplied to it, or absorbed from it, by a suitable power supply or sink. In the UPFC arrangement the real power of the SVS exchanges is provided by one of the end buses (e.g., the sending-end bus), as indicated in the figure 2. (This arrangement conforms to the objective of controlling the power flow by the UPFC rather than increasing the generation capacity of the system.)

In the presently used practical implementation, the UPFC consists of two voltage-sourced converters using five level NPC multilevel inverter, as illustrated in Figure 1. five level NPC multilevel inverter is shown in fig 3. These converters, are operated from a common dc link provided by a dc storage capacitor. This arrangement functions as an ideal ac to ac power converter in which the real power can freely flow in either direction between the ac terminals of the two converters, and each converter can independently generate (or absorb) reactive power at its own ac output terminal.

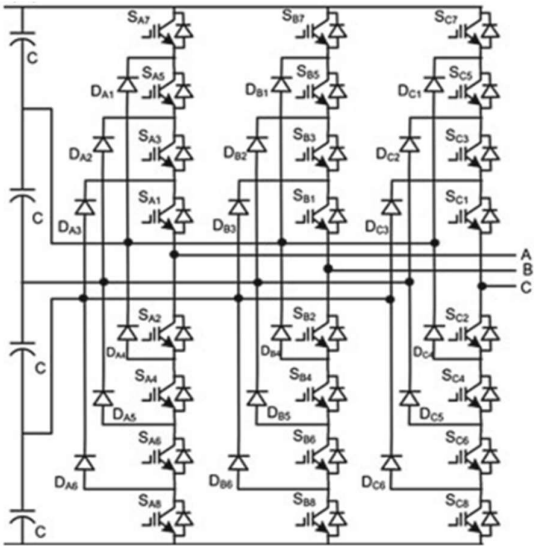

Fig.3. Three-phase five level NPC power converter

Series converter provides the main function of the UPFC by injecting a voltage with controllable magnitude u_pq and phase angle ρ in series with the line via an insertion transformer. This injected voltage acts essentially as a synchronous ac voltage source. The transmission line current flows through this voltage source resulting in reactive and real power exchange between it and the ac system. The reactive power exchanged at the ac terminal (i.e., at the terminal of the series insertion transformer) is generated internally by the converter. The real power exchanged at the ac terminal is converted into dc power which appears at the dc link as a positive or negative real power demand.

The basic function of Shunt converter is to supply or absorb the real power demanded by Series converter at the common dc link. This dc link power is converted back to ac and coupled to the transmission line via a shunt-connected transformer. Shunt converter can also generate or absorb controllable reactive power, if it is desired, and thereby provide independent shunt reactive compensation for the line. It is important to note that whereas there is a closed "direct1 ' path for the real power negotiated by the action of series voltage injection through series and shunt converters back to the line, the corresponding reactive power exchanged is supplied or absorbed locally by Series converter and therefore does not have to be transmitted by the line. Thus, Shunt converter can be operated at a unity power factor or be controlled to have a reactive power exchange with the line independent of the reactive power exchanged by Series converter. This means that there is no reactive power flow through the UPFC.

Viewing the operation of the Unified Power Flow Controller from the standpoint of traditional power transmission based on reactive shunt compensation, series compensation, and phase shifting, the UPFC can fulfill all these functions and thereby meet multiple control objectives by adding the injected voltage u_pq, with appropriate amplitude and phase angle, to the (sending-end) terminal voltageu_s.

(a) Voltage regulation

(b) Line impedance compensation

(c) Phase shifting

(d) Simultaneous control of voltage, impedance and angle

Voltage regulation with continuously variable in-phase/anti-phase voltage injection, shown at

a for voltage increments u_pq=±Δu(ρ =0). Functionally this is obtainable with a transformer tap-changer having infinitely small steps. Series reactive compensation is shown at b where u_pq=u_qis injected in quadrature with the line current. Functionally this is like, but more general than the controlled series capacitive and inductive line compensation. This is because the UPFC injected series compensating voltage can be kept constant, if desired, independent of line current variation, whereas the voltage across the series compensating (capacitive or inductive) impedance varies with the line current.

Phase shifting (transmission angle regulation) where u_pq=u_q is injected with an angular relationship with respect to u_s that achieves the desired σ phase shift (advance or retard) without any change in magnitude. Thus, the UPFC can function as a perfect phase shifter. From the practical viewpoint, it is also important to note that, in contrast to conventional phase shifters, the ac system does not have to supply the reactive power the phase shifting process demands since it is internally generated by the UPFC converter. Multi-function power flow control, executed by simultaneous terminal voltage regulation, series capacitive line compensation, and phase shifting whereu_pq=Δu+u_q+u_σ This functional capability is unique to the UPFC. No single conventional equipment has similar multi-functional capability.

The general power flow control capability of the UPFC, from the viewpoint of conventional transmission control, can be illustrated best by the real and reactive power transmission versus transmission angle characteristics of the simple two machine system. With reference to this figure 2, the transmitted power P and the reactive power -jQ_r, supplied by the receiving-end, can be expressed as follows:

$$P - jQ_r = u_r\left(\frac{u_s + u_{pq} - u_r}{jX}\right)^* \tag{6}$$

where symbol * means the conjugate of a complex number and j = √(-1) If u_pq=0 ,then equation (7) describes the uncompensated system, that is,

$$P - jQ_r = u_r\left(\frac{u_s - u_r}{jX}\right)^* \tag{7}$$

Thus, with u_pq≠0, the total real and reactive power can be written in the form:

$$P - jQ_r = u_r\left(\frac{u_s - u_r}{jX}\right)^* + \frac{u_r u_{pq}\,*}{-jX} \tag{8}$$

Substituting

$$u_s = ue^{j\frac{\delta}{2}} = u\left(\cos\frac{\delta}{2} + j\sin\frac{\delta}{2}\right) \tag{9}$$

$$u_r = ue^{-j\frac{\delta}{2}} = u\left(\cos\frac{\delta}{2} - j\sin\frac{\delta}{2}\right) \tag{10}$$

and

$$u_{pq} = u_{pq}e^{j\left(\frac{\delta}{2}+\rho\right)} = u_{pq}\left\{\cos\left(\frac{\delta}{2}+\rho\right) + \sin\left(\frac{\delta}{2}+\rho\right)\right\} \tag{11}$$

the following expressions are obtained for P and Q_r:

$$P(\delta,\rho) = P_o(\delta) + P_{pq}(\rho) = \frac{u}{X}\sin\delta - \frac{uu_{pq}}{X}\cos\left(\frac{\delta}{2}+\rho\right) \tag{12}$$

And

$$Q_r(\delta,\rho) = Q_{or}(\delta) + Q_{pq}(\rho) = \frac{u^2}{X}(1 - cos\delta) - \frac{uu_{pq}}{X}\sin\left(\frac{\delta}{2}+\rho\right) \tag{13}$$

Where

$$P_O(\delta) = \frac{u^2}{X} sin\delta, Q_{or} = -\frac{u^2}{X}(1 - cos\delta) \tag{14}$$

are the real and reactive power characterizing the power transmission of the uncompensated system at a given angle δ . Since angle ρ is freely variable between 0 and 2πat any given transmission angle δ(0≤δ≤π), it follows that P_pq (ρ) and Q_pq (ρ) are controllable between-(uu_pq)/Xand (+uu_pq)/X independent of angle δ . Therefore, the transmittable real power P is controllable betweenand the reactive power is controllable between at any transmission angle S, as illustrated

$$P_o(\delta) - \frac{uu_{pq}}{X} \le P_o(\delta) + \frac{uu_{pq}}{X},\ Q_o(\delta) - \frac{uu_{pq}}{X} \le Q_o \le Q_o(\delta) + \frac{uu_{pq}}{X} \tag{15}$$

B. Shunt Inverter Control

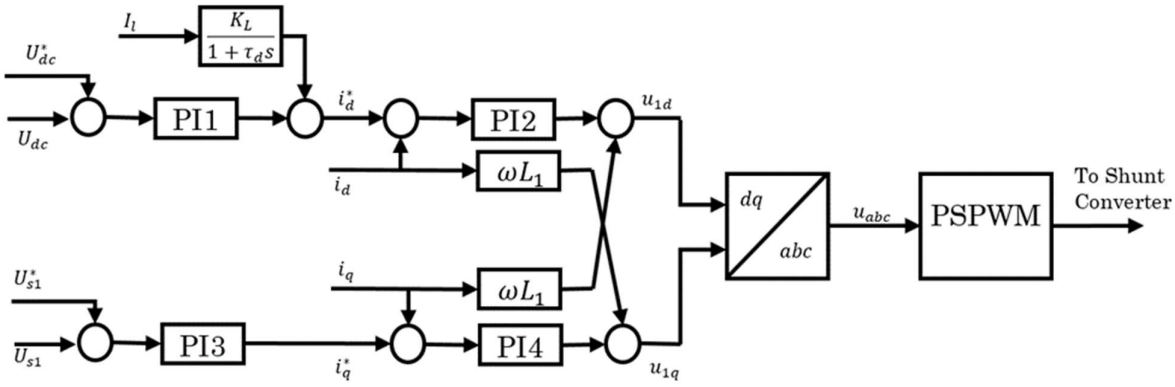

Fig4. Shunt Inverter Control

The shunt converter regulates the shunt reactive power, but mainly controls the dc-link voltageU_dC=U_dcref , supplying or absorbing the active power demanded by the series converter to keep constant the common dc-link voltageU_dC. Since the ac currents of the shunt inverter present fast dynamics compared to the slow dynamics of the dc-link voltage, the two shunt converter tasks must determine, respectively:

The i_d^*shunt current is suitable to keep constant the dc bus voltage level, using PI controller.

The i_q^* reference current suitable to keep constant the line voltage magnitude, using PI controller

$$i^*_d = k_{p1}(U_{dC} - U^*_{dc}) + k_{i1}\int_0^t (U_{dC} - U^*_{dc})dt + I_l\left(\frac{K_L}{1+\tau_d s}\right) \tag{16}$$

$$i^*_q = k_{p3}(U_{s1} - U^*_{s1}) + k_{i3}\int_0^t (U_{s1} - U^*_{s1})dt \tag{17}$$

$$u_{1d} = k_{p2}(i^*_d - i_d) + k_{i2}\int_0^t (i^*_d - i_d)dt + i_q\omega L \tag{18}$$

$$u_{1q} = k_{p4}(i^*_q - i_q) + k_{i4}\int_0^t (i^*_q - i_q)dt - i_d\omega L \tag{19}$$

B. Series Inverter Real-Time PWM Controller

To control the active and reactive power in the transmission line, the series inverter must supply a series voltage with appropriate magnitude and angle. The inverter output voltages are nonlinear time variant τ_rfunctions of the dc-link capacitor voltages, which can be disturbed during line faults. To gain insensitivity to these disturbances, instead of a preprogrammed pulse width-modulator (PWM) generator relying on the dc-link voltage nominal value, the series

inverter output voltage PWM is computed in real time so that the dc-link voltage variations are considered and do not impair the PF to be enforced by the series converter. Failure to produce the desired PFs could lead to transmission system shut down. PWM generation methods ensure that voltage pulses must have the same volt-second average of the fundamental sinusoidal (i.e., the time integral of the n-level voltage waveform minus the value of the sinusoidal should be zero). Therefore, to real time compute the PWM, a switching period is chosen, where the output voltages V_cRd,V_cRQ are used to generate pulses required by five level NPC inverter of series converter.

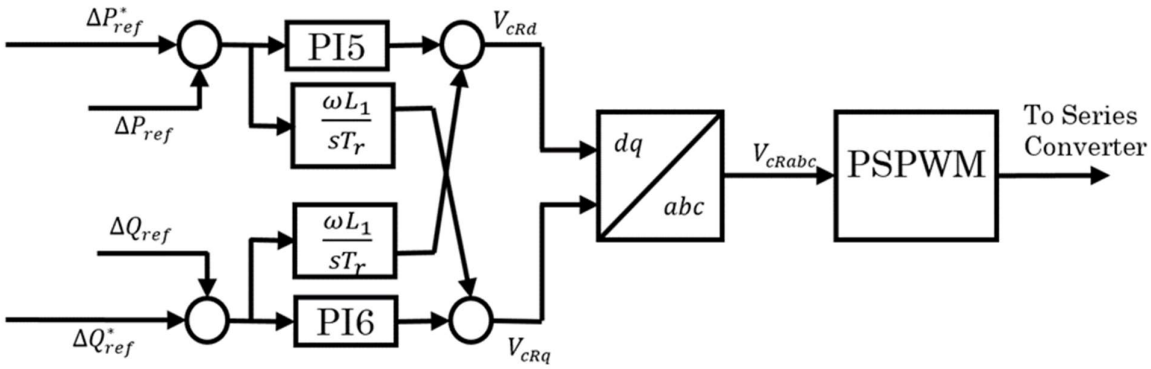

Fig.5. Series Converter PF controller block diagram

$k_{p1}, k_{i1}, k_{p2}, k_{i2}, k_{p3}, k_{i3}, k_{p4}, and\ k_{i4}$, of shunt converter and k_p5,k_i5,k_p6,and k_i6 of seroes converter are PI controller gains of the control system. These gains are optimized by using trial and error methods. The disadvantages of trial and error tuned PI controllers are that it gives rise to a higher maximum deviation, a longer response time and a longer period of oscillation than with other intelligent controllers. This type of control action is therefore used where the above can be tolerated and offset is undesirable. Hence Particle Swarm Optimization is adopted to optimize the PI controller gains of UPFC control system.

3. Grey Wolf Optimizer (GWO)

3.1. Inspiration

Grey wolf (Canis lupus) belongs to the Canidae family. Grey wolves are considered apex predators, meaning that they are at the top of the food chain. Grey wolves mostly prefer to live in a pack. The group size is 5–12 on average. Of particular interest is that they have a very strict socially dominant hierarchy as shown in Fig. 6. The leaders are a male and a female, called alphas. The alpha is mostly responsible for making decisions about hunting, sleeping place, time to wake, and so on. The alpha's decisions are dictated to the pack. However, democratic behavior has also been observed, in which an alpha follows the other wolves in the pack. The entire pack acknowledges the alpha in gatherings by holding their tails down. The alpha wolf is also called the dominant wolf since his/her orders should be followed by the pack. The alpha wolves are only allowed to mate in the pack. Interestingly, the alpha is not necessarily the strongest member of the pack but the best in terms of managing the pack. This shows that the organization and discipline of a pack is much more important than its strength.

The second level in the hierarchy of grey wolves is beta. The betas are subordinate wolves that help the alpha in decision-making or other pack activities. The beta wolf can be either male or female, and he/she is probably the best candidate to be the alpha in case one of the alpha wolves

passes away or becomes very old. The beta wolf should respect the alpha but commands the other lower-level wolves as well. It plays the role of an advisor to the alpha and discipliner for the pack. The beta reinforces the alpha's commands throughout the pack and gives feedback to the alpha. The lowest ranking grey wolf is omega. The omega plays the role of scapegoat. Omega wolves always must submit to all the other dominant wolves. They are the last wolves that are allowed to eat. It may seem the omega is not an important individual in the pack, but it has been observed that the whole pack faces internal fighting and problems in case of losing the omega. This is due to the venting of violence and frustration of all wolves by the omega(s). This assist satisfying the entire pack and maintaining the dominance structure. In some cases, the omega is also the babysitters in the pack.

If a wolf is not an alpha, beta, or omega, he/she is called subordinate (or delta in some references). Delta wolves must submit to alphas and betas, but they dominate the omega. Scouts, sentinels, elders, hunters, and caretakers belong to this category. Scouts are responsible for watching the boundaries of the territory and warning the pack in case of any danger. Sentinels protect and guarantee the safety of the pack. Elders are the experienced wolves who used to be alpha or beta. Hunters help the alphas and betas when hunting prey and providing food for the pack. Finally, the caretakers are responsible for caring for the weak, ill, and wounded wolves in the pack. In addition to the social hierarchy of wolves, group hunting is another interesting social behavior of grey wolves. According to Muro et al. the main phases of grey wolf hunting are as follows:

Tracking, chasing, and approaching prey.

Pursuing, encircling, and harassing the prey until it stops moving.

Attack towards the prey.

In this work this hunting technique and the social hierarchy of grey wolves are mathematically modeled to design GWO and perform optimization.

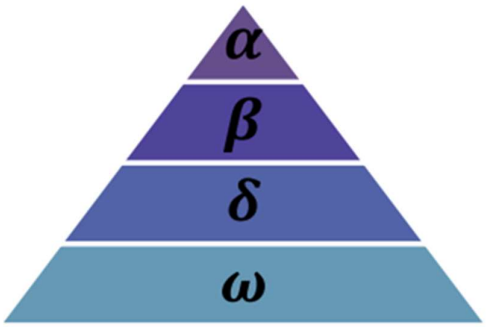

Fig6. Hierarchy of grey wolf (dominance decreases from top down).

3.2. Mathematical model and algorithm

3.2.1. Social hierarchy

To mathematically model the social hierarchy of wolves when designing GWO, we consider the fittest solution to be the alpha (α). Consequently, the second and third best solutions are named beta (β) and delta (δ) respectively. The rest of the candidate solutions are assumed to be omega (ω). In the GWO algorithm, the hunting (optimization) is guided by α, β, and δ. The ω wolves follow these three wolves.

3.2.2. Encircling prey

As mentioned above, grey wolves encircle prey during the hunt. To mathematically model encircling behavior the following equations are proposed:

$$\vec{D} = \left|\vec{C}.\vec{X}_p(t) - \vec{X}(t)\right| \quad (20)$$

$$\vec{X}(t+1) = \vec{X}_p(t) - \vec{A}.\vec{D} \quad (21)$$

where t indicates the current iteration, A ⃗ and C ⃗ are coefficient vectors,X ⃗_p (t) is the position vector of the prey, and X ⃗ indicates the position vector of a grey wolf.

The vectors A ⃗ and C ⃗ are calculated as follows:

$$\vec{A} = 2\vec{a}.\vec{r}_1 - \vec{a} \quad (22)$$

$$\vec{C} = 2\vec{r}_2 \quad (23)$$

where components of a ⃗ are linearly decreased from 2 to 0 over the course of iterations and r_1, r_2 are random vectors in [0, 1].

To see the effects of Eqs. (3.1) and (3.2), a two-dimensional position vector and some of the possible neighbors are illustrated in Fig. 7(a). As can be seen in this figure, a grey wolf in the position of (X, Y) can update its position according to the position of the prey (X^*, Y^*). Different places around the best agent can be reached with respect to the current position by adjusting the value of $\vec{A}\ and\ \vec{C}$ vectors. For instance, $(X^* - X,\ Y^*)$can be reached by setting $\vec{A} = (1,0);$ and $\vec{C} = (1,1)$. The possible updated positions of a grey wolf in 3D space are depicted in Fig. 7(b). Note that the random vectors $r_1\ and\ r_2$ allow wolves to reach any position between the points illustrated in Fig. 7. So, a grey wolf can update its position inside the space around the prey in any random location by using Eqs. (3.1) and (3.2). The same concept can be extended to a search space with n dimensions, and the grey wolves will move in hyper-cubes (or hyper-spheres) around the best solution obtained so far.

Fig. 7. Hunting behavior of grey wolves: (A) chasing, approaching, and tracking prey (B–D) pursuiting, harassing, and encircling (E) stationary situation and attack.

3.2.3. Hunting

Grey wolves can recognize the location of prey and encircle them. The hunt is usually guided by the alpha. The beta and delta might also participate in hunting occasionally. However, in an abstract search space we have no idea about the location of the optimum (prey). To mathematically simulate the hunting behavior of grey wolves, we suppose that the alpha (best candidate solution) beta, and delta have better knowledge about the potential location of prey. Therefore, we save the first three best solutions obtained so far and oblige the other search

agents (including omegas) to update their positions according to the position of the best search agents. The following formulas are proposed in this regard.

$$\vec{D}_\alpha = \left|\vec{C}_1.\vec{X}_\alpha - \vec{X}\right| \tag{24}$$

$$\vec{D}_\beta = \left|\vec{C}_2.\vec{X}_\beta - \vec{X}\right| \tag{25}$$

$$\vec{D}_\delta = \left|\vec{C}_3.\vec{X}_\delta - \vec{X}\right| \tag{26}$$

$$\vec{X}_1 = \vec{X}_\alpha - A_1\vec{D}_\alpha \tag{27}$$

$$\vec{X}_2 = \vec{X}_\beta - A_2\vec{D}_\beta \tag{28}$$

$$\vec{X}_3 = \vec{X}_\delta - A_3\vec{D}_\delta \tag{29}$$

$$\vec{X}(t) = \frac{\vec{X}_1 + \vec{X}_2 + \vec{X}_3}{3} \tag{30}$$

Fig. 7 shows how a search agent updates its position according to alpha, beta, and delta in a 2D search space. It can be observed that the final position would be in a random place within a circle which is defined by the positions of alpha, beta, and delta in the search space. In other words, alpha, beta, and delta estimate the position of the prey, and other wolves update their positions randomly around the prey.

3.2.4. Attacking prey (exploitation)

As mentioned above the grey wolves finish the hunt by attacking the prey when it stops moving. To mathematically model approaching the prey we decrease the value of a $\vec{}$. Note that the fluctuation range of A $\vec{}$ is also decreased by a $\vec{}$. In other words,A $\vec{}$ is a random value in the interval [-2a,2a] where a is decreased from 2 to 0 over the course of iterations. When random values of A $\vec{}$ are in [-1,1], the next position of a search agent can be in any position between its current position and the position of the prey. Fig. 8(a) shows that |A| < 1 forces the wolves to attack towards the prey. With the operators proposed so far, the GWO algorithm allows its search agents to update their position based on the location of the alpha, beta, and delta; and attack towards the prey. However, the GWO algorithm is prone to stagnation in local solutions with these operators. It is true that the encircling mechanism proposed shows exploration to some extent, but GWO needs more operators to emphasize exploration.

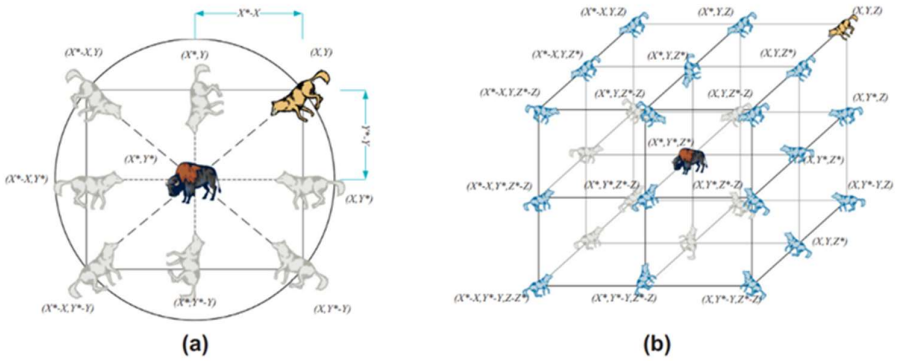

(a) (b)

Fig. 8. 2D and 3D position vectors and their possible next locations.

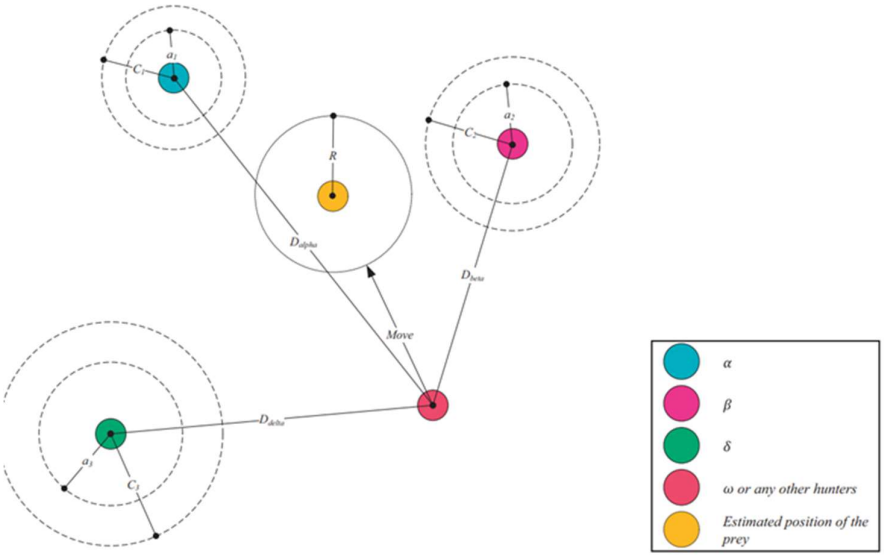

Fig. 9. Position updating in GWO.

3.2.5. Search for prey (exploration)

Grey wolves mostly search according to the position of the alpha, beta, and delta. They diverge from each other to search for prey and converge to attack prey. To mathematically model divergence, we utilize $\vec{A}$ with random values greater than 1 or less than -1 to oblige the search agent to diverge from the prey. This emphasizes exploration and allows the GWO algorithm to search globally. Fig. 9(b) also shows that $|A| > 1$ forces the grey wolves to diverge from the prey to hopefully find a fitter prey.

Another component of GWO that favors exploration is $\vec{C}$. As may be seen in Eq. (3.4), the $\vec{C}$ vector contains random values in [0,2]. This component provides random weights for prey to stochastically emphasize ($C > 1$) or deemphasize ($C < 1$) the effect of prey in defining the distance in Eq. (3.1). This assists GWO to show a more random behavior through optimization, favoring exploration and local optima avoidance. It is worth mentioning here that C is not linearly decreased in contrast to A. We deliberately require C to provide random values at all timesto emphasize exploration not only during initial iterations but also final iterations. This component is very helpful in case of local optima stagnation, especially in the final iterations.

The C vector can be also considered as the effect of obstacles to approaching prey in nature. The obstacles in nature appear in the hunting paths of wolves and in fact prevent them from quickly and conveniently approaching prey. This is exactly what vector C does. Depending on the position of a wolf, it can randomly give the prey a weight and make it harder and farther to reach for wolves, or vice versa. To sum up, the search process starts with creating a random population of grey wolves (candidate solutions) in the GWO algorithm. Over the course of iterations, alpha, beta, and delta wolves estimate the probable position of the prey. Each candidate solution updates its distance from the prey. The parameter a is decreased from 2 to 0 to emphasize exploration and exploitation, respectively. Candidate solutions tend to diverge from the prey when$|\vec{A}|>1$ and converge towards the prey when$|\vec{A}|<1$. Finally, the GWO algorithm is terminated by the satisfaction of an end criterion.

The pseudo code of the GWO algorithm is presented. To see how GWO is theoretically able to solve optimization problems, some points may be noted:

The proposed social hierarchy assists GWO to save the best solutions obtained so far over the course of iteration.

The proposed encircling mechanism defines a circle-shaped neighborhood around the solutions which can be extended to higher dimensions as a hyper-sphere.

The random parameters A and C assist candidate solutions to have hyper-spheres with different random radii.

The proposed hunting method allows candidate solutions to locate the probable position of the prey.

Exploration and exploitation are guaranteed by the adaptive values of a and A.

The adaptive values of parameters a and A allow GWO to smoothly transition between exploration and exploitation.

With decreasing A, half of the iterations are devoted to exploration ($|A| \geq 1$) and the other half are dedicated to exploitation ($|A| < 1$).

The GWO has only two main parameters to be adjusted (a and C).

There are possibilities to integrate mutation and other evolutionary operators to mimic the whole life cycle of grey wolves. However, we have kept the GWO algorithm as simple as possible with the fewest operators to be adjusted. Such mechanisms are recommended for future work.

Pseudocode of GWO algorithm

Pseudocode of GWO algorithm

1. **Initialization of number of candidates or grey wolves n, Number of Iterations ite**
2. **Initialize $a, \vec{A}$ and $\vec{C}$**
3. **for $i = 1$ to n**
4. **Initialize $G = \{s_1, s_2, \dots, s_n\}$ randomly within the range of $\{lb, ub\}$**
5. **end for**
6. **Evaluate or find fitness value of each candidate or grey wolf $f(G)$**
7. **Grade the candidates with respect to their fitness values such as X_α the best solution, X_β the second-best solution and X_δ the third best solution**
8. **While (stop criterion is not satisfied and $ite <$ $maximum\ number\ of\ iterations$) do**
9. **for $i = 1$ to n**
10. **update the position of candidates by using Eq. []**
11. **end for**
12. **renew $a, \vec{A}$ and $\vec{C}$**
13. **Evaluate the function using each candidate and grade them**
14. **Renew the position of X_α, X_β and X_δ**
15. **Ite=ite+1**
16. **end while**

In the UPFC control system of shunt converter and series converter there are six proportional gains (K_p1 to K_p6)and six integral constants (K_i1 to K_i6). The challenge is to determine all these constants for the UPFC to provide optimal active and reactive power control and voltage regulation. To do this for the power system in Fig. 1 , the active and reactive power errors, voltage magnitude error, DC link voltage error and current errors are used as the

measure of performance of the shunt and series VSI controls. To arrive at the twelve optimal parameters using the Grey Wolf Optimization, twenty PSO particles are selected each providing a stable dynamic and transient UPFC control. The PSO algorithm minimizes the following cost function.

$$Cost = \sum_{t=0}^{20000} \left(\sqrt{(\Delta P_{error}(t))^2} + \sqrt{(\Delta Q_{error}(t))^2} + \sqrt{(\Delta U_{dc}(t))^2} + \sqrt{(\Delta U_{s1}(t))^2} + \sqrt{(\Delta i_d(t))^2} + \sqrt{(\Delta i_q(t))^2} \right) \quad (31)$$

Where ΔP_error, ΔQ_error are active and reactive power errors, ΔU_dc is DC link voltage error,ΔU_s1 voltage magnitude error and Δi_d and Δi_q are direct and quadrature axis current errors. The cost is calculated and minimized to optimize PI controller gains of control system.

V. SIMULATION RESULTS

To authenticate the dynamic performance of the proposed NPC based five level GWO optimized UPFC control, the test network model of Fig. 1 with the shown parameters in table1 is simulated. Generators are modeled by three phase synchronous machines with exciters, driven by hydraulic turbine with governors, power stabilizers, and an output transformer. The selected test transmission network topology represents a system part with a 220-kV subsystem in parallel with another220-KV subsystemi.e. double circuit transmission line.

Table I. Parameters of The test System

Sending end	Synchronous Machine 1000MVA, 13.8KV, 50Hz Transformer 1000MVA, 13.8KV/220KV
Receiving end	Synchronous Machine 1200MVA, 13.8KV, 50Hz Transformer 1200MVA, 13.8KV/220KV
Line L1	Resistance 0.068 Ω/km Inductance 1.31 mH/km Capacitance 0.00885 μF/km Line Length 65km
Line L2	Resistance 0.068 Ω/km Inductance 1.31 mH/km Capacitance 0.00885 μF/km Line Length 65km
UPFC	DC Link Voltage 56KV DC Link Capacitors each 750 μF Shunt Converter rating 100MVA Series Converter rating 100MVA

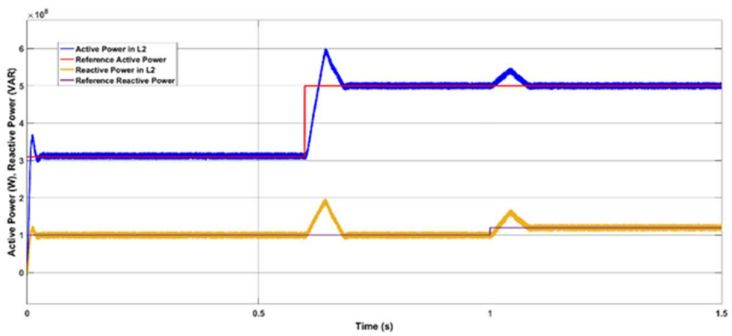

(a)

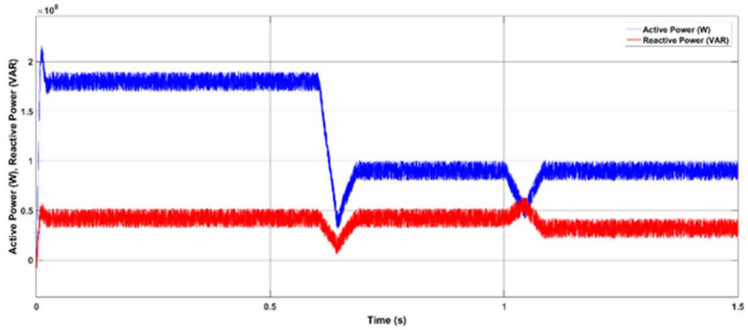

(b)

Fig.10. Step response of the UPFC controlled system with PI: (a) active and reactive power in the UPFC line L2 (b) active and reactive power in line L1,

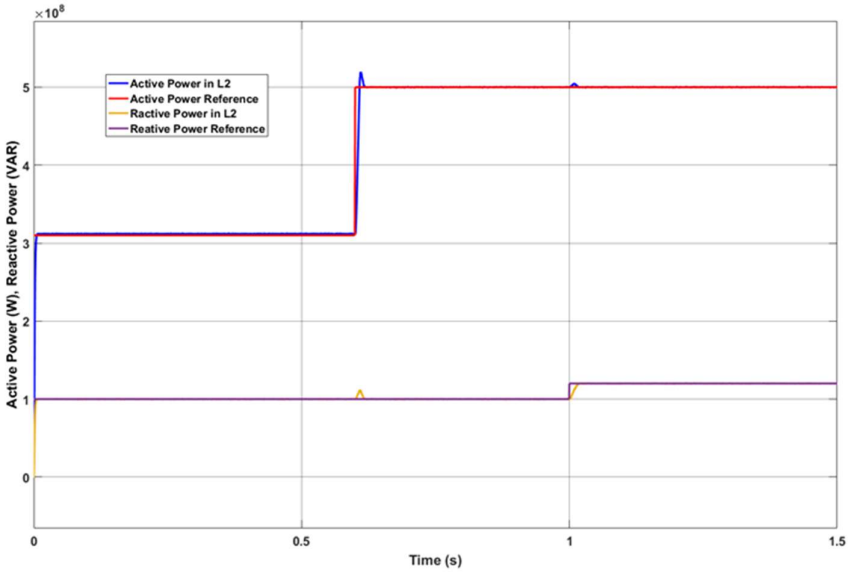

(a)

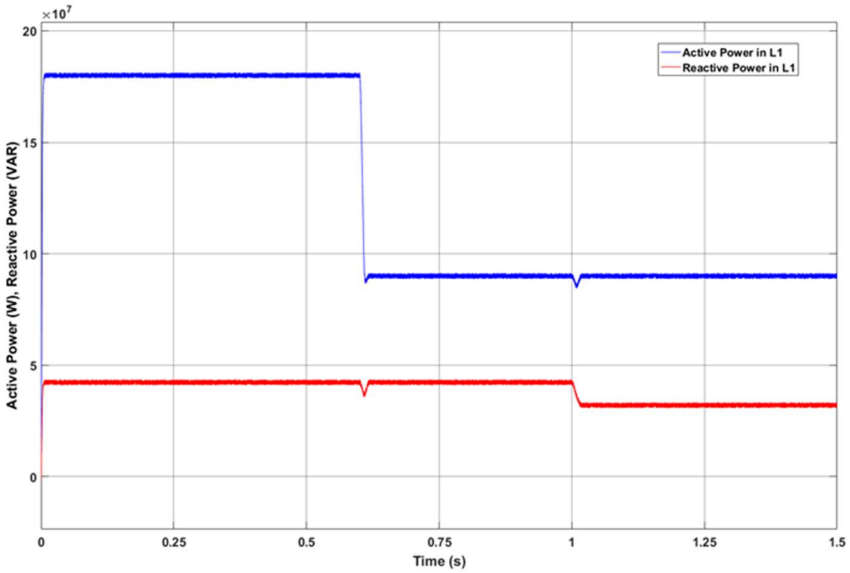

(b)

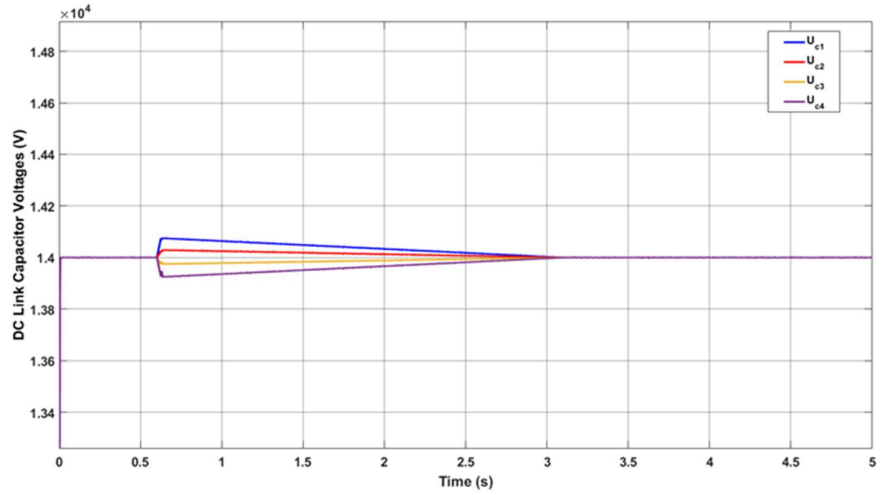
×10^4
DC Link Capacitor Voltages (V)
Time (s)
U_c1
U_c2
U_c3
U_c4

(c)

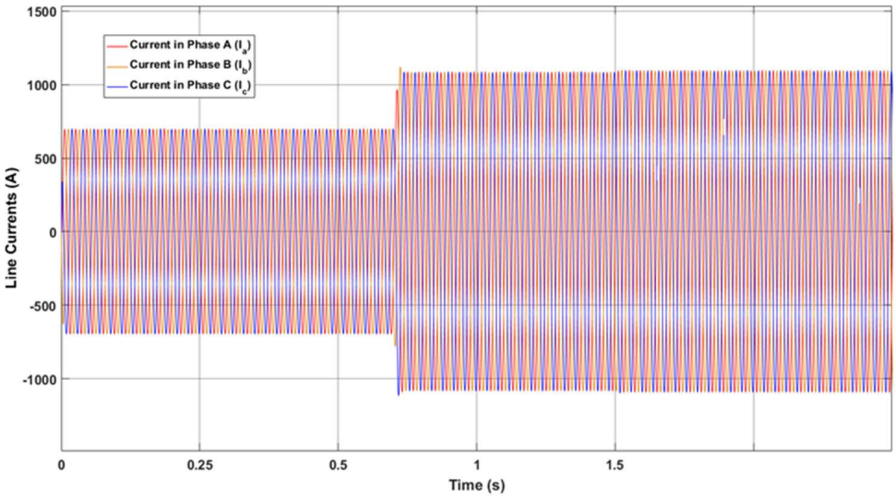
Line Currents (A)
Time (s)
Current in Phase A (I_a)
Current in Phase B (I_b)
Current in Phase C (I_c)

(d)

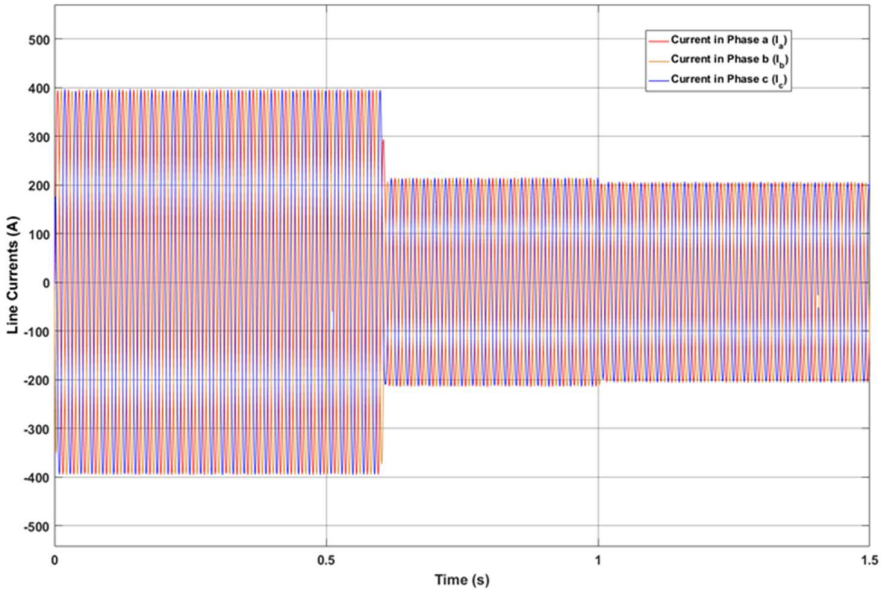
Line Currents (A)
Time (s)
Current in Phase a (I_a)
Current in Phase b (I_b)
Current in Phase c (I_c)

(e)

Fig.11. Step response of the UPFC controlled system with GWO tuned PI: (a) active and reactive power in the UPFC lineL_2 , (b) active and reactive power in one of the L_1 lines, and (c) dc-link capacitor voltages waveforms (d) Li line Currents (e) L2 Line Currents

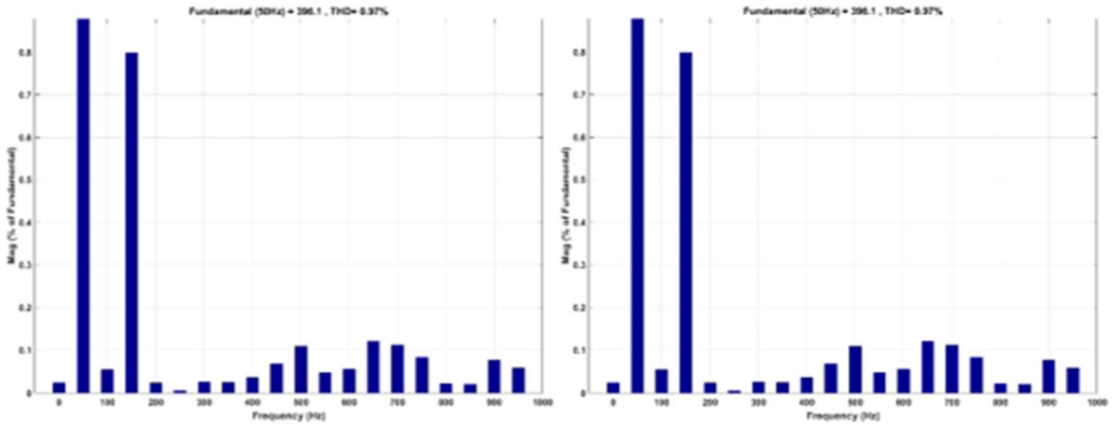

(a) (b)

Fig.12. Total Harmonic Distortion of L1 and L2 line currents

The UPFC is connected in betweenbuses 2 and 4 in Line 2. For a constant power flow between sending end to receiving end through double circuit transmission line, regulation of power in Line 2, where UPFC is connected, controls the power flow in Line 1.Two Five level NPC converters are connected in back-to-back connection as series and shunt converters. Phase shifted pulsewidth modulation is adopted to generate the switching pulses required by both converters.In case of series converter, reference wave forms required by PSPWM are generated from DC voltage control and line voltage magnitude control. In case of shunt converter, reference wave forms required by PSPWM are generated from active and reactive power control. To test the controllers, the converter models, including semiconductor switching, were built in the Matlab/Simulink environment within the network. In a first test, the system dynamic response to a step change in active and reactive power references for the second 220-kV line, controlled by the UPFC, was investigated. Initial values were P=312 MW and Q_ref=90.00 MVAr. Steps are applied at t=0.6 s for P_ref=500.00 MW and at t=1 s for 120.00 MVAr. Initially UPFC is tested on double circuit transmission line with PI controller gains which are tuned by using trial and error method. These gains are tabulated in table 1. Active and reactive power flow in line L2 and L1 are depicted in fig 10(a) and (b) in which peak over shoot and stability time are 20% and 0.12 seconds respectively.

Due to this poor performance of PI controller in UPFC in terms of peak overshoot and stability time, system can become unstable during dynamic conditions. To improve the tracking capacity of PI controllers, GWO is adopted to tune the gains.The proposed method mimicked the social hierarchyand hunting behavior of grey wolves. Gains which are optimized using GWO optimization are presented in table II. Active and reactive power flow in line L2 and L1 are depicted in fig 11(a) and (b). Voltages across DC link capacitors of five level multilevel inverter are presented in fig 11(c). line currents in line L1 and line L2 are presented in fig11(d) and fig11(e). fig 13presents THD of line L1 and L2 currents. As seen in fig 11, active reactive power tracking by UPFC in Line L2 is improved due to GWO optimization in terms of peak

overshoot and stability time.

A three-phase fault is simulated in one of the 220-kV double lines (L2) at 0.6 s, being cleared at 0.64 s, assuming a line outage. Fig 12, fig 13 and fig 14depict the active and reactive power flow in L1 and L2 lines without UPFC, with normal PI controlled UPFC and with GWO optimized PI controlled UPFC. Fig. 12(a) and 13(b) shows the active and reactive power flows, without using the UPFC, in the healthy line L1 in parallel with the faulty line L2. During the three-phase fault, the transmitted power is nearly zero, but after the fault is cleared, line L_1 is overloaded. Using the multilevel UPFC, this line's active and reactive PFs can be controlled in line (L2). Fig 13(a) and 13(b) present the active and reactive power flows in line L1 and L2 with normal PI controller. Fig 14(a) and 14(b) present the active and reactive power flows in line L1 and L2 with GWO optimized PI controller. As can be seen from this figure, after the fault is cleared, the power transfer in this line will be controlled by the UPFC to maintain the active and reactive PF capacity limits of the line L1.

In fig 15 performance of GWO optimized PI controller is examined using dynamic conditions of active and reactive power change. Active power is change in the sequence of 310 MW, 500 MW, 400 MW, 300 MW and 500 MW at the timing sequence of 0, 0.6, 1.5, 2.2 and 3 seconds respectively.Reactive power is change in the sequence of 100 MW, 150 MW and 100 MW at the timing sequence of 0, 1 and 3 seconds respectively. As seen from fig 14 tracking capacity of proposed GWO optimized PI controller is efficient and alsopeak overshoot and stability time are reduced.

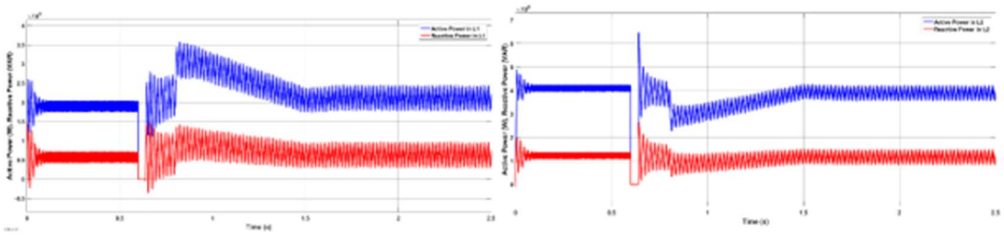

(a) (b)

Fig 13. Active and reactive power in L1 and L2 without UPFC

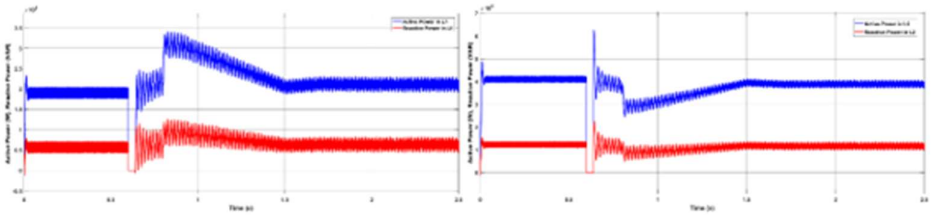

(a) (b)

Fig 14. Active and reactive power in L1 and L2 with PI controlled UPFC

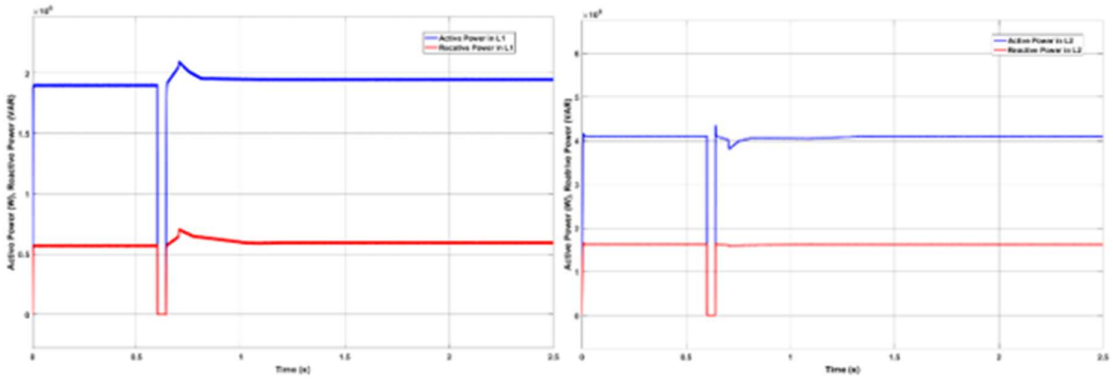

(a) (b)

Fig 15. Active and reactive power in L1 and L2 with GWO tuned PI controlled UPFC

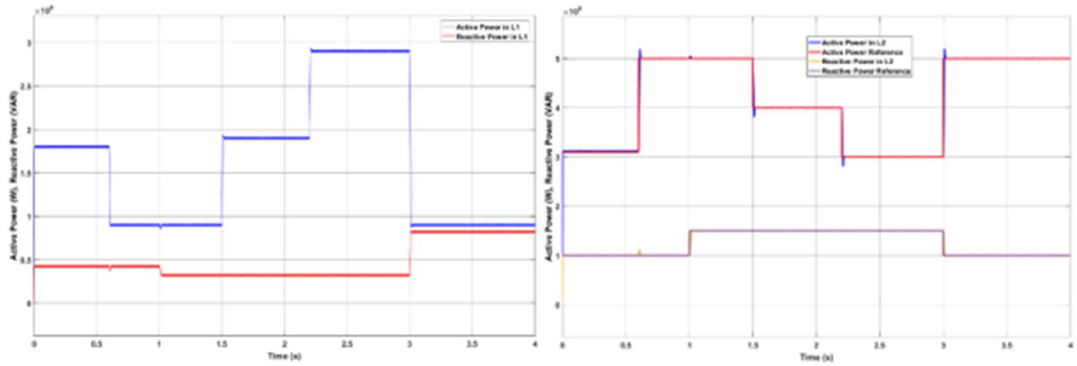

(a) (b)

Fig 16. Active and Reactive power in L1 and L2 line during reference change

Table 2. PI Controller Gains

Using Trial and Error method	**K_{p1}=0.1285, K_{p2}=0.6740, K_{p3}=1.0852, K_{p4}=0.9052, K_{p5}=2.3851, K_{p6}=1.1850, K_{i1}=6.7581, K_{i2}=10.0857, K_{i3}=3.8570, K_{i4}=2.0745, K_{i5}=3.6857, K_{i6}=5.0745**
Using GWO optimization	**K_{p1}=0.0135, K_{p2}=0.1958, K_{p3}=0.8044, K_{p4}=0.9875, K_{p5}=2.8077, K_{p6}=0.7095, K_{i1}=7.4251, K_{i2}=14.0147, K_{i3}=4.4785, K_{i4}=2.1085, K_{i5}=6.1785, K_{i6}=4.4089**

VI.CONCLUSIONS

This paper proposes GWO optimization for tuning of PI controller of UPFC which controls active and reactive power flow in double circuit transmission line. Two five level NPC multilevel converters are adopted as shunt and series converters which are connected in back-to-back. The proposed UPFC control strategy includes: 1) decoupled active and reactive linear power control; 2) real-time PWM generation in both UPFC multilevel converters, dc-link voltage control gains with low sensitivity to dc link current, and 3) the balancing of the dc-link capacitor voltages using both multilevel converters. The dc-link capacitor voltages, which are usually balanced using only one of the multilevel converters, are balanced using both series

and shunt multilevel converters, the results shows that the proposed technique with GWO gives better results. Optimization by GWO for PI controller gains improves tracking capacity of active and reactive power flow.

REFERENCES

Abbate.L, M. Trovato, C. Becker and E.Handschin, "Advanced Steady-State Models of UPFC for Power System Studies IEEE 2002 pp .449-454.

L. Gyugyi, C. D. Schauder, and K. K. Sen, "Static synchronous series compensator: A solid-state approach to the series compensation of transmission lines," IEEE Trans. Power Delivery, vol. 12, no. 1, pp. 406–413, 1997.

Fuerte-Esquivel C.R, E. Acha "Unified power flow controller: a critical comparison of Newton-Raphson UPFC algorithms in power flow studies" IEE Proc.-Gener. Transm. Distrib., Vol. 144, No. 5, September 1997

Soesanti, I., Syahputra, R. (2016). Batik Production Process Optimization Using Particle Swarm Optimization Method. Journal of Theoretical and Applied Information Technology (JATIT), 86(2), pp. 272-278.

Jamal, A., Syahputra, R. (2014). Power Flow Control of Power Systems Using UPFC Based on Adaptive Neuro Fuzzy. IPTEK Journal of Proceedings Series. 2014; 1(1): pp. 218-223.

H. Akagi, Y. Kanazawa, and A. Nabae, "Instantaneous reactive power compensators comprising switching devices without energy storage components," IEEE Trans. Ind. Applicat., vol. 20, no. 3, pp. 625–630, 1984.

Lashkar Ara A, Kazemi A and NabaviNiaki SA (2011) Modelling of optimal unified power flow controller (OUPFC) for optimal steady-state performance of power systems. Energy Conversion and Management 52(2): 1325–1333

Ghadimi N, Afkousi-Paqaleh A and Emamhosseini A (2013) A PSObased fuzzy long-term multi-objective optimization approach for placement and parameter setting of UPFC. Arabian Journal for Science and Engineering 39(4): 2953–2963.

] M. Mustapha, B. U. Musa, and M. U. M. Bakura, "Modelling of unified power flow controller (UPFC) for the control of real and reactive power flow on 500kV interconnected power system," Proc. University of Maiduguri Faculty of Engineering Lecture Series, vol. 6, pp. 98-105, Dec. 2015.

Z. Anwar, T. N. Malik, and T. Abbas, "Power flow and transient stability enhancement using thyristor controlled series compensation," Mehran University Research Journal of Engineering & Technology, vol. 37, no. 4, pp. 685-700, 2018.

B.A. Renz, A. Keri, A.S. Mehraben, C. Schauder, E. Stacey, I. Kovalsky, L. Gyugui, and A. Edris, 1999, "AEP Unified Power Flow Controller Performance", IEEE Trans. On Power Delivery, 14(4), pp. 1374-1381.

Li, P., Ji, H., Wang, C., Zhao, G., Song, G., Ding, F., Wu, J.: Coordinated control method of voltage and reactive power for active distribution networks based on soft open point. IEEE Trans. Sustain. Energy 8(4), 1430–1442 (2017)

G. Kenne et al., "A New Hybrid UPFC Controller for Power Flow Control and Voltage Regulation Based on RBF Neuro sliding Mode Technique," Advances in Electrical Engineering, vol. 5, pp. 44–48,

B. Benazza, H. Ouadi, and F. Giri, "Output feedback control of a three-phase four-wire unified power quality conditioner," Asian Journal of Control, vol. 22, no. 3, pp. 1147–1162, 2020.

Gholipour, E. and Saadate, S. (2005) 'Improving of transient stability of power systems usingUPFC', Transactions on Power Delivery, April, IEEE, Part 2, Vol. 20, No. 2, pp.1677–1682.

Bouhali, O., François, B., Berkouk, E.M. and Sandemont, C.S. (2007) 'DC link capacitor inthree-phas diode clamped inverter controlled by direct space vector of line-to-line voltages',IEEE Trans. on Power Electronics, Vol. 22, No. 5, pp.1636–1648.

Wang HF. Application of modeling UPFC into multi-machine power systems. IEE Proc Gen TransmDistrib 1999;146(3):306–12.

Moe MoeOo and Myint Thuzar, "Transmission Capacity Improvement Using Unified Power Flow Controller with New Control Strategy," International Journal of Electrical and Electronic Engineering & Telecommunications, vol. 10, no. 3, pp. 225-232, May 2021.

Krishna, P. Gopi, and T. Gowri Manohar. "Available transfer capability computations in deregulated power system with the optimal location of unified power flow controller." International Journal of Electrical and Electronics Engineering Research (IJEEER) 2.3 (2012): 121-138.

Rao, D., and Rama Chadra. "Enhancement Of Power Quality Using Mc-Dpfc In Transmission System." International Journal of Electrical and Electronics Engineering Research (IJEEER) 6.6: 1 12 (2016).

Gandhi, Ronak, Gajendra Patel, and Harshkumar Sharma. "SIMULATION OF DISTRIBUTED POWER FLOW CONTROLLER FACTS DEVICE IN VOLTAGE SAG AND SWELL MITIGATION." International Journal of Electrical and Electronics Engineering Research (IJEEER) 7 (2017): 39-44.

Mahela, Om Prakash, and Sheesh Ram Ola. "Optimal capacitor placement for loss reduction in electric transmission system using genetic algorithm." TJPRC-International Journal of Electrical and Electronics Engineering Research 3.2 (2013): 59-68.